Plant Mol Biol (2015) 88:119–131
DOI 10.1007/s11103-015-0312-3

The cytosolic branched-chain aminotransferases of *Arabidopsis thaliana* influence methionine supply, salvage and glucosinolate metabolism

Kurt Lächler[1] · Janet Imhof[1] · Michael Reichelt[2] · Jonathan Gershenzon[2] · Stefan Binder[1]

Received: 9 January 2015 / Accepted: 22 March 2015 / Published online: 8 April 2015

Abstract *Arabidopsis thaliana* possesses six branched-chain aminotransferases (BCAT1–6). Previous studies revealed that some members of this protein family are involved in the biosynthesis of branched-chain amino acids and/or in the Met chain elongation pathway, the initial steps towards the biosynthesis of Met-derived glucosinolates. We now analyzed branched-chain aminotransferase 6 (BCAT6). In vivo GFP-tagging experiments strongly suggest this enzyme to be localized to the cytosol. Substrate specificity assays performed with recombinant enzyme revealed that BCAT6 transaminates Val, Leu and Ile as well as the corresponding 2-oxo acids but also transaminates Met and its cognate ketoacid 4-methyl-2-oxobutanoate. We established single (*bcat6-1*), double (*bcat4-2*/*bcat6-1*) and triple (*bcat3-1*/*bcat4-2*/*bcat6-1*) mutants involving BCAT6 with the latter exhibiting a clear macroscopic phenotype with smaller plants and abnormal leaf morphology. Metabolite profiling of these mutants demonstrated that BCAT6 can contribute to Met chain elongation with the triple mutant line lacking BCAT3, 4 and 6 showing a dramatic reduction of Met-derived glucosinolate species down to 32 and 14 % of wild-type levels in plant foliage and seeds, respectively. This drop in glucosinolate levels is accompanied by a 46-fold increase of free Met, demonstrating the important role of the three branched-chain aminotransferases in converting Met to its 2-oxo acid for glucosinolate chain elongation. In addition, we determined the relative amounts of 5′-deoxy-5′-methylthioadenosine, an intermediate of the Met recycling pathway. This metabolite accumulated to relative high amounts in the absence of the cytosolic BCAT4 and BCAT6, suggesting that cytosolic Met salvage also contributes to the biosynthesis of glucosinolates.

Keywords *Arabidopsis thaliana* · Amino acids · Glucosinolates · Branched-chain aminotransferases

Introduction

The three amino acids Val, Leu and Ile, called branched-chain amino acids (BCAAs), are characterized by their small aliphatic hydrocarbon side chains (Binder 2010; Singh 1999). These amino acids are essential for humans and animals, which depend on external sources for these compounds such as bacteria, fungi or plants. In the latter organisms, BCAAs are de novo synthesized in chloroplasts. Biosynthesis follows two parallel pathways involving a common set of four enzymes, which catalyze the formation of Val from two molecules of pyruvate and Ile from pyruvate and 2-oxobutanoate, which is obtained by the deamination of Thr. The committed step of BCAA biosynthesis is catalyzed by acetohydroxyacid synthase, a heterodimer composed of a large catalytic and small regulatory subunit, through which the activity of the enzyme is inhibited by BCAAs. Acetohydroxyacid synthase is also the target for commercially important herbicides such as the sulfonylureas and imidazolinones (Wittenbach and Abell 1999). In two following reactions, catalyzed by ketolacid reducto-isomerase and

Electronic supplementary material The online version of this article (doi:10.1007/s11103-015-0312-3) contains supplementary material, which is available to authorized users.

✉ Stefan Binder
Stefan.binder@uni-ulm.de

[1] Institut Molekulare Botanik, Universität Ulm, Albert-Einstein-Allee 11, 89069 Ulm, Germany

[2] Abteilung Biochemie, Max Planck Institut für Chemische Ökologie, Hans-Knöll-Straße 8, Beutenberg Campus, 07745 Jena, Germany

dihydroxyacid dehydratase, the 2-oxo acids 3-methyl-2-oxobutanoate (3MOB) and 3-methyl-2-oxopentanoate (3MOP) are formed. While the latter is transaminated to Ile, 3MOB can either be converted into Val or it can be used for the synthesis of Leu. The biosynthesis of Leu starts out with the formation of isopropylmalate (IPM) formed by a condensation reaction combining acetyl-CoA with 3MOB. This reaction is catalyzed by isopropylmalate synthase. Two additional steps involving isopropylmalate isomerase (IPMI) and isopropylmalate dehydrogenase form 4-methyl-2-oxopentanoate (4MOP), a 2-oxo acid elongated by a methylene group. Finally 4MOP is transaminated to Leu involving a branched-chain aminotransferase.

The final transamination reactions, which convert the 2-oxo acids into Val, Leu or Ile, are catalyzed by branched-chain aminotransferases (BCATs). In *Arabidopsis thaliana* (Arabidopsis) six transcribed members (BCAT1–6) and an apparently un-transcribed pseudo gene (BCAT7) form the small BCAT gene family (Diebold et al. 2002). While the mitochondrial BCAT1 and BCAT2 seem to function in BCAA degradation (Angelovici et al. 2013; Schuster and Binder 2005), the chloroplast-located BCAT3 is involved in the biosynthesis of BCAAs, predominantly Val (Knill et al. 2008). One of the characteristics of the BCATs is their promiscuity which extends their substrate range to compounds such as α-aminobutyrate and more importantly Met. The cytosolic BCAT4 exhibits a particularly unusual substrate spectrum. This enzyme has apparently lost its original function in BCAA metabolism and instead is involved in the biosynthesis of Met-derived aliphatic glucosinolates (Schuster et al. 2006). Accordingly it has affinities to Met and its 2-oxo acid, 4-methylthio-2-oxobutanoate (MTOB), whereas it exhibits only marginal activity with Leu and no activity at all with Val and Ile. Glucosinolates are a group of heterogeneous specialized metabolites synthesized from different amino acids (Halkier and Gershenzon 2006; Wittstock and Halkier 2002). Accordingly they are classified as indolic (Trp), benzenic (Tyr and Phe) and aliphatic glucosinolates, which are synthesized from Ala, Val, Leu and Ile but predominantly from Met.

The biosynthesis of Met-derived glucosinolates is divided into three phases. In the first phase, the Met chain elongation pathway, Met is elongated by one or several methylene groups to obtain homo-methionine and other Met derivatives. This includes a reaction cascade identical to the one required for the elongation of 3MOB to 4MOP in Leu biosynthesis. Furthermore, the enzymes catalyzing these reactions can be involved in both Met chain elongation and Leu biosynthesis. For instance, the large subunit of the isopropylmalate isomerase (IPMI LSU) has a dual function (Knill et al. 2009). By forming heterodimers with different small subunits it participates in Leu biosynthesis (together with IPMI SSU1) or participates in Met chain elongation (together with IPMI SSU2 or 3). The chloroplast-located BCAT3 also plays a role in Met chain elongation in addition to its function in BCAA biosynthesis (Knill et al. 2008). Besides the Met chain elongation pathway, a transamination reaction affecting Met occurs also in the Met salvage pathway. *S*-adenosylmethionine (SAM) is used as a substrate for ethylene biosynthesis. Within this pathway 5′-deoxy-5′-methylthioadenosine (5MTA) is produced as by-product, which is recycled to Met formed in the last reaction by the transamination of MTOB (Miyazaki and Yang 1987; Sauter et al. 2013).

To obtain a complete picture about the biological roles of the individual members of the BCAT gene family in Arabidopsis, we have now investigated BCAT6. This protein was shown to reside in the cytosol and to accept all BCAAs, Met and the corresponding 2-oxo acids as substrates. A detailed metabolite analysis of single, double and triple mutants suggests multiple functions of BCAT6 in this model species.

Materials and methods

Plant cultivation

Arabidopsis thaliana (Arabidopsis) plants were grown as described before (Knill et al. 2008; Schuster et al. 2006). Knockout mutants were obtained from the SALK Institute for Biological Studies (*bcat6-1*, SALK119840) or from the INRA Centre (*bcat6-2*, FLAG062B04 and *bcat6-3*, FLAG365E01). Double and triple knockouts were established from previously characterized *bcat3-1* (GABI-Kat 002A11) and *bcat4-2* (GABI-Kat 163D11) mutants (Knill et al. 2008; Schuster et al. 2006) following standard protocols (Weigel and Glazebrook 2002). Seedlings were also grown on plates with Murashige and Skoog (MS) medium containing 0.5 % (w/v) sucrose.

Overexpression, purification and substrate specificity tests

The BCAT6 reading frame was amplified from total oligo(dT)-primed cDNA with the primer pair bcat6UE.H/bcat6UE.R, digested with *BamHI*/*Xho*I, and cloned into the corresponding sites of pET32a (Novagen). Overexpression was induced in *Escherichia coli* strain AD494(DE3)pLysS by the addition of 1 mM IPTG and cells were grown for 4.5 h at 37 °C under constant shaking at 200 rpm. Purification of recombinant BCAT6 protein was done by His-tag affinity chromatography using Ni-NTA Superflow Resin (Qiagen). BCAT6 protein in the enriched fractions was quantified using AIDA Image Analyzer v3.12 (Raytest, Germany) in Coomassie Blue-stained SDS gels. The

amount of recombinant BCAT6 in the protein fraction used for activity tests was found to be about 66 %. All enzyme activity and substrate specificity tests were performed with 6.5 µg of protein from a single His-Tag-purified fraction in a total volume of 50 µl for 20 min at 37 °C in the presence of 100 mM Bicine pH 8.3, 100 µM pyridoxal-5-phosphate and 5 mM DTT. Reactions were initiated by adding 1 µl of enzyme preparation corresponding to 4.26 µg recombinant BCAT6 protein. Kinetic studies with Leu, Ile, Val, Met and the corresponding 2-oxo acids were conducted with substrate concentrations between 0.25 and 15.0 mM in the presence 5.0 mM 2-oxoglutarate or 5.0 mM glutamic acid as co-substrates. Reactions were terminated by heat denaturation at 94 °C for 10 min. After precolumn derivatization with *o*-phthaldialdehyde/2-mercaptoethanol the reaction products were quantified by reversed phase high performance liquid chromatography using a SUPELCOSIL LC-18-DB column (Supelco). For quantifying the deamination of amino acids by BCAT6, the amount of glutamic acid formed in the reaction was measured in the samples. Calculation of V_{max} and K_m was done using the Origin 7.0 software (OriginLab).

Metabolite analysis

Glucosinolates were quantified as described previously (Imhof et al. 2014; Knill et al. 2008; Schuster et al. 2006). Amino acids and other metabolites such as Leu-derivatives, 5′-deoxy-5′-methylthioadenosine (5MTA) and 1-amino-5-benzoyloxypentane (5BZO-NH_2) were measured in 10 mg of seeds or 20 mg of freeze-dried leaves. Amino acids were extracted with 1 ml of 80 % (v/v) methanol solution and the resulting extract was diluted in a ratio of 1:10 (v:v) in water containing the ^{13}C, ^{15}N labelled amino acid mix (Isotec, Miamisburg, OH, USA). Amino acids in the diluted extracts were directly analyzed by LC–MS/MS as described before with the modification that an API5000 mass spectrometer (Applied Biosystems) was used and the chromatographic gradient was modified as following: 0–1 min, 3 % B in A; 1–3.8 min, 3–50 % B in A; 3.8–3.9 min, 50–100 % B in A; 3.9–5 min 100 % B, 5.0–5.1 min, 100–3 % B in A, and 5.1–7.5 min 3 % B in A, (A: 0.05 % formic acid in water; B: acetonitrile) (Docimo et al. 2012). Parameters for the analysis of additional analytes by LC–MS/MS are listed in Supplemental Table S1. Structures of these metabolites were given in Supplemental Figure S1.

Analysis of subcellular localization

The *BCAT6* reading frame was amplified with the oligonucleotide pair bcat6-EGFP.H/bcat6-EGFP.R and cloned into the *Sgs*I/*Pac*I restriction sites of vector pMDC32 containing 2× CaMV 35S promoter and a NOS terminator. The reading frame of the enhanced green fluorescent protein (EGFP) was amplified using the primer pair EGFP.H/EGFP.R on vector pSAT6-EGFP-N1 as template and cloned into *Sac*I/*Pac*I restriction sites in frame at the C-terminus of the *BCAT6* reading frame. The construct was checked by DNA sequencing (LGC Genomics) and transformed into the *bcat6-1* mutant following an established protocol (Clough and Bent 1998). After selection of transformants on MS plates containing 15 µg/ml hygromycin, leaf protoplasts were prepared and inspected as outlined previously (Matthes et al. 2007). In addition, C- and N-terminal fusions of BCAT6 were cloned in pSAT6—EYFP-C1 or pSAT6—EYFP-N1 vectors (Tzfira et al. 2005). Protoplast preparation, transformation and inspection were done as described (Matthes et al. 2007). Fluorescence microscopy was performed with an Axio Observer Z1 microscope equipped with camera system AxioCam MRm (Carl Zeiss AG) and the following filter sets: Zeiss filter sets 46 HE YFP, EX BP 500/25, BS FT 515, EM BP 535/30 and 38 HE eGFP, EX BP 470/40, BS FT 495, EM BP 525/50.

Miscellaneous methods

Basic methods of molecular biology were performed according to standard protocols (Sambrook and Russell 2001). Total RNA was extracted from 15 to 20 d-old plants using the Spectrum Plant Total RNA Kit (Sigma-Aldrich). Total cellular DNA was isolated from 10 to 20 d-old plants as described in a previously established protocol (Edwards et al. 1991). Various pSAT6 vectors were obtained from the Arabidopsis Biological Resource Center (ABRC, Columbus, OH, USA). DNA sequencing was obtained commercially (LGC Genomics). Histochemical GUS staining was performed according to a protocol described previously modified by the addition of 0.05 % (v/v) Silwet Top (www.agrar.basf.at/). Images were taken using a Bresser Advance ICD 10 – 160 stereo microscope equipped with MikroCamII 3.1 MP digital camera (www.bresser.de). Oligonucleotide sequences are given in Supplemental Table S2.

Results

Branched-chain aminotransferase 6 (BCAT6) is a cytosolic enzyme

The subcellular localization of BCAT6 (At1g50110) has not been previously studied, but the enzyme has been assumed to be localized in the cytosol since it lacks potential N-terminal extensions. To address this localization experimentally the complete *BCAT6* reading frame was cloned in-frame upstream or downstream of the gene

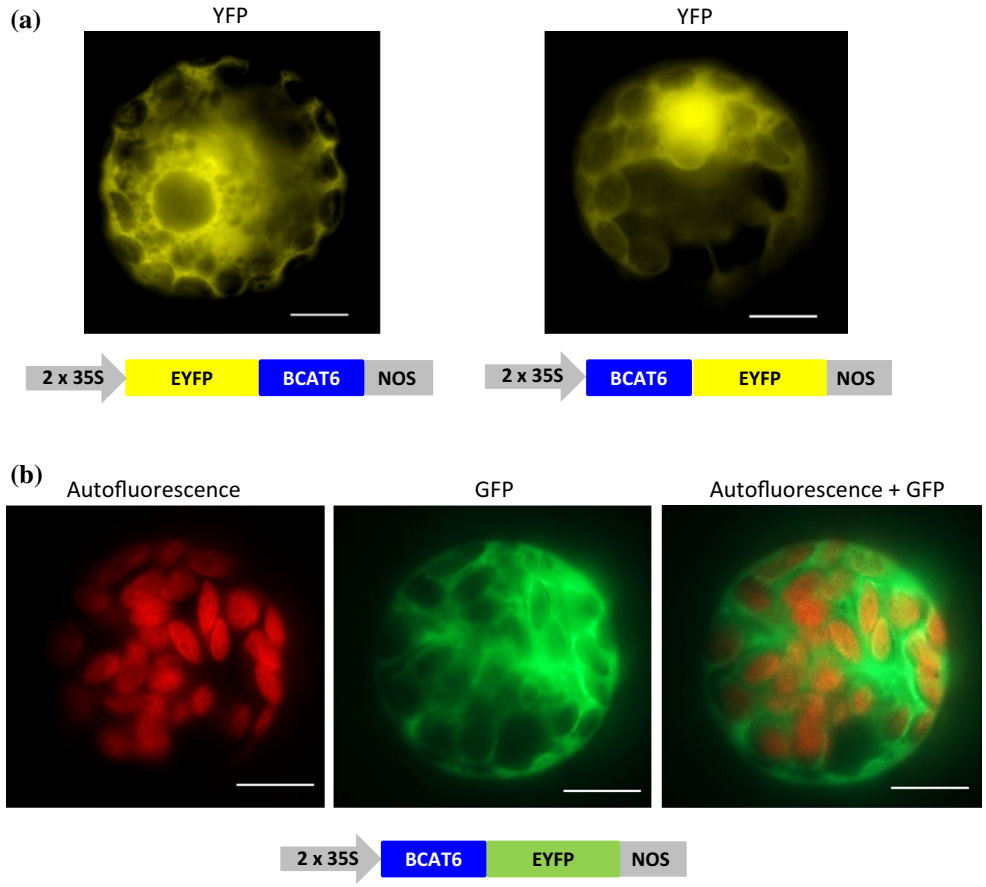

Fig. 1 Subcellular localization of BCAT6. **a** Transient expression of enhanced yellow fluorescent (EYFP) protein:BCAT6 fusions in tobacco protoplasts. Constructs are illustrated beneath the images. **b** An Arabidopsis protoplast released from a plant expressing a BCAT6: enhanced green fluorescent protein (EGFP) fusion. A simplified scheme of the construct is given in the *bottom*. Autofluorescence of the chlorophyll or EGFP fluorescence are detected separately (*left* and *middle panel*) or together (*right panel*). The *scale bar* corresponds to 10 µm

encoding the yellow fluorescent protein (YFP). These constructs were established in the pUC19 vector and used for transient transformation of tobacco protoplasts. As expected, the yellow fluorescence was observed in the cytosol, particularly with the construct in which the *BCAT6* reading frame was fused to the C-terminus of the YFP gene (Fig. 1a, left panel). With BCAT6 located upstream of the YFP gene, localization was also observed in the cytosol, but the BCAT6:EYFP fusion protein might also slightly accumulate in the nucleus (Fig. 1a, right panel). To substantiate these results, we designed another construct in which BCAT6 was fused to the N-terminus of EGFP. This chimeric gene was established in the vector pMDC32, which allowed a stable introduction of the transgene via *Agrobacterium* into Arabidopsis. After selection of transformants, several different plant lines were established and investigated by epifluorescence microscopy. To this end, individual cells were released from the rosette leaf tissue of 21 d-old plants. Inspection of the protoplasts again revealed a diffuse distribution of the green fluorescence in the cytosol, which is consistent with the results observed with the transiently expressed fusion proteins. In both approaches fluorescence was never seen in chloroplasts, mitochondria or peroxisomes. Collectively, these data strongly suggest a localization of BCAT6 in the cytosol. Thus Arabidopsis contains two cytosolic BCATs, BCAT4 which catalyzes the committed step in the methionine chain elongation pathway of glucosinolate biosynthesis (Schuster et al. 2006), and BCAT6.

BCAT6 shows highest affinity towards Ile and 3-methyl-2-oxopentanoate (3MOP)

To get information about the substrate spectrum of BCAT6 we performed kinetic studies with recombinant BCAT6 protein and the three BCAAs and Met as well as the corresponding 2-oxo acids (Supplemental Fig. S2). For all substrates except for 4-methylthio-2-oxobutanoate (MTOB),

Table 1 BCAT6 substrate specificity

Amino acid	K_m (mM)	V_{max} [µmol (min mg)$^{-1}$]	2-Oxo acid	K_m (mM)	V_{max} [µmol (min mg)$^{-1}$]
Met	6.58 ± 0.69	2.90 ± 0.15	MTOB	2.83 ± 0.99*	1.39 ± 0.17*
Leu	3.34 ± 0.56	2.06 ± 0.13	4MOP	2.64 ± 0.42	1.02 ± 0.06
Val	4.41 ± 0.43	2.34 ± 0.10	3MOB	2.69 ± 0.39	0.78 ± 0.04
Ile	3.27 ± 0.63	2.05 ± 0.15	3MOP	1.08 ± 0.24	0.68 ± 0.04

* Reactions with MTOB did not follow a typical Michaelis–Menten kinetic. *Abbreviations 3MOB* 3-methyl-2-oxobutanoate, *3MOP* 3-methyl-2-oxopentanoate, *4MOP* 4-methyl-2-oxopentanoate, *MTOB* 4-methylthio-2-oxobutanoate

plotting of the reaction velocities and the substrate concentration revealed Michaelis–Menten kinetics. K_m and V_{max} were calculated by fitting the data into non-linear regression (Table 1). Generally higher K_m-values were calculated for amino acids in comparison to their cognate 2-oxo acids. All K_m-values were in a range found in previous studies of BCATs in Arabidopsis and tomato (Knill et al. 2008; Maloney et al. 2010; Schuster and Binder 2005). Consistent with previous results obtained by yeast complementation assays (Diebold et al. 2002), BCAT6 converts all BCAAs and their corresponding 2-oxo acids to their respective transamination products. This substrate range clearly differentiates BCAT6 from BCAT4, which lacks substantial activities with Val, Ile and the corresponding 2-oxo acids 3-methyl-2-oxobutanoate (3MOB) and 3-methyl-2-oxopentanoate (3MOP) (Schuster et al. 2006). The highest affinity of BCAT6 was seen with Ile and its 2-oxo acid, 3-methyl-2-oxopentanoate (3MOP).

In contrast to all other substrates investigated, the reaction velocities measured with MTOB did not exhibit classical Michaelis–Menten kinetics (Supplemental Fig. S2). Here activities increased to a maximum at 8 mM substrate concentration, but further elevation of the MTOB concentration led to a decrease of activity. In any case, both Met and MTOB are substrates of BCAT6 consistent with the generally promiscuous character of branched-chain aminotransferases in plants.

The knockout of BCAT6 moderately alters the glucosinolate profile in Arabidopsis

To evaluate the biological role of BCAT6 in vivo, we established three T-DNA knockout mutants. Two of these mutants (*bcat6-2*, FLAG062B04 and *bcat6-3*, FLAG365E01) were in the Wassilewskija (Ws) nuclear background whereas one T-DNA insertion line (*bcat6-1*, SALK 119840) was generated in the accession Columbia (Col-0). By PCR analysis and sequencing of the corresponding products, the localization of the T-DNA was confirmed at the end of the second exon (*bcat6-1* and *bcat6-3*) or in intron 2 (*bcat6-2*). An RT-PCR analysis with oligonucleotides flanking the insertion confirmed the knockout of BCAT6 in these lines (Supplemental Fig. S3). The macroscopic phenotypes of all of these mutants were indistinguishable from wild-type plants (Fig. 2 and Supplemental Fig. S4). For comparability with previous studies of other BCATs from Arabidopsis, which were done in the Col-0 background, we concentrated our studies on the *bcat6-1* line.

Profiling of free amino acids in *bcat6-1* did not reveal any significant changes from the wild-type control both in leaves (Table 2, Supplemental Table S3) and in seeds (Table 3, Supplemental Table S4), except for Trp, which was slightly increased in the seeds. Since in Arabidopsis BCATs might also have functions in glucosinolate biosynthesis, we also measured these compounds. In leaves, only minor decreases of 7-methylsulfinylheptylglucosinolate (7MSOH) and 8-methylsulfinyloctylglucosinolate (8MSOO) were measured (Supplemental Table S5). In seeds, 4-benzoyloxybutylglucosinolate (4BZO) was slightly decreased, but in contrast to leaves, 7-methylthioheptylglucosinolate (7MTH), 8-methylthiooctylglucosinolate (8MTO) and 8-methylsulfinyloctylglucosinolate were found to be moderately increased (Table 5, Supplemental Table S6). In summary, the moderate changes of C7 and C8 glucosinolate species both in leaves and seeds suggest a participation in or at least an indirect influence of BCAT6 on the Met chain elongation pathway.

Inactivation of both BCAT6 and BCAT4 leads to effects on both free amino acid and glucosinolate contents

To investigate the effects of the knockout of both cytosolic BCATs, we crossed the *bcat6-1* plants with the previously characterized *bcat4-2* knockout mutant (Schuster et al. 2006). Like the single mutants, the macroscopic phenotype of the double knockout (dko) plants was indistinguishable from that of the Col-0 wild type (Fig. 2). On the other hand, a number of differences were seen between the metabolite profile of the *bcat4-2*/*bcat6-1* dko and that of Col wild-type as well as the single mutants. In leaves, Met, Ser, Val and *S*-methylmethionine (SMM) were increased in the dko (Table 2, Supplemental Table S3). SMM is synthesized from Met and SAM in a Met-SAM-methyltransferase

Fig. 2 Macroscopic phenotypes of single and multiple mutants with T-DNA insertions in *BCAT6*, *BCAT4* and *BCAT3*. 21 d-old (**a**) and 42 d-old (**b**) plants were grown under long-day conditions. Leaves of the *bcat3-1/bcat4-2/bcat6-1* triple mutant plants showed dents (**c**) and sometimes chlorosis at the leaf edge (**d**)

Table 2 Amino acid levels in leaves of various *bcat* mutants

Amino acid	Amino acid content in leaves (μmol/g dry weight)					
	Col-0	*bcat6-1*	*bcat4-2*	*bcat3-1*	*bcat4-2/bcat6-1*	*bcat3-1/bcat4-2/bcat6-1*
Ile	0.41 ± 0.03	0.39 ± 0.03	0.43 ± 0.04	0.34 ± 0.01*	0.45 ± 0.03	0.55 ± 0.05*,†
Leu	0.30 ± 0.01	0.27 ± 0.03	0.30 ± 0.05	0.40 ± 0.04*	0.29 ± 0.02	0.66 ± 0.05*,†
Val	1.11 ± 0.14	1.17 ± 0.11	1.09 ± 0.07	0.57 ± 0.04*	1.30 ± 0.08*	0.68 ± 0.06*,†
Met	0.40 ± 0.08	0.45 ± 0.05	2.19 ± 0.33*	0.60 ± 0.09*	2.28 ± 0.26*	18.49 ± 1.70*,†
SMM	0.24 ± 0.04	0.19 ± 0.03	0.68 ± 0.12*	0.17 ± 0.02*	0.74 ± 0.07*	1.37 ± 0.16*,†
Total	183.66 ± 28.99	187.76 ± 18.24	180.04 ± 11.41	177.51 ± 10.99	196.17 ± 11.35	224.02 ± 8.84

Values for all amino acids are given in Supplemental Table S2

* $p < 0.01$ in a statistical *t* test between Col-0 and the mutants

† $p < 0.01$ between *bcat4-2/bcat6-1* and *bcat3-1/bcat4-2/bcat6-1*

catalyzed reaction. SMM serves a methyl donor for the formation of Met from homocysteine, a reaction catalyzed by homocysteine *S*-methyltransferase. Met-SAM-methyltransferase and homocysteine *S*-methyltransferase form the SMM cycle, which controls the Met-SAM balance (Ranocha et al. 2001). For Met and SMM, elevations could be mainly attributed to the knockout of *bcat4-2*, although they were stronger in the *bcat4-2/bcat6-1* dko (Table 2). On the other hand, the significantly higher levels of Val and Ser in the dko most likely arose from an additive effect of both gene knockouts, since the single mutants exhibited only insignificant increases of these amino acids. In seeds,

Table 3 Levels of free amino acids in seeds of *bcat* mutants

Amino acid	Amino acid content in seeds (µmol/g dry weight)					
	Col-0	*bcat6-1*	*bcat4-2*	*bcat3-1*	*bcat4-2/bcat6-1*	*bcat3-1/bcat4-2/bcat6-1*
Ile	0.22 ± 0.07	0.20 ± 0.02	0.43 ± 0.22	0.26 ± 0.04	0.53 ± 0.20*	1.72 ± 0.36*,†
Leu	0.11 ± 0.05	0.08 ± 0.02	0.15 ± 0.04	0.12 ± 0.03	0.18 ± 0.05	0.46 ± 0.04*,†
Val	0.40 ± 0.26	0.49 ± 0.23	0.43 ± 0.05	0.38 ± 0.04	0.47 ± 0.13	1.29 ± 0.06*,†
Met	0.09 ± 0.02	0.09 ± 0.01	0.09 ± 0.01	0.11 ± 0.02	0.20 ± 0.06*	0.41 ± 0.06*,†
SMM	n. d.	n. d.	0.50 ± 0.86	n. d.	1.54 ± 0.08*	3.50 ± 0.29*,†
Total	17.61 ± 3.44	17.36 ± 1.17	24.41 ± 2.66*	21.01 ± 1.69	20.70 ± 2.55	39.26 ± 2.38*,†

Values for all amino acids are given in Supplemental Table S3

n.d.: not detectable

* $p < 0.01$ in a statistical *t* test between Col-0 and the mutants

† $p < 0.01$ between *bcat4-2/bcat6-1* and *bcat3-1/bcat4-2/bcat6-1*

Table 4 Glucosinolate content in foliage of diverse *bcat* mutants

Glucosinolate	Glucosinolate content in leaves (µmol/g dry weight)					
	Col-0	*bcat6-1*	*bcat4-2*	*bcat3-1*	*bcat4-2/bcat6-1*	*bcat3-1/bcat4-2/bcat6-1*
Met-derived						
4MSOB	16.14 ± 1.29	15.38 ± 0.91	9.81 ± 0.56*	12.10 ± 0.94*	7.99 ± 0.33*	4.06 ± 0.26*,†
Total	22.80 ± 1.57	21.44 ± 1.18	12.14 ± 0.65*	20.38 ± 1.40	9.83 ± 0.38*	7.33 ± 0.38*,†
Leu-derived						
4MP	n. d.	n. d.	n. d.	1.76 ± 0.18*	n. d.	2.83 ± 0.06*,†
5MH	n. d.	n. d.	n. d.	0.67 ± 0.05*	n. d.	6.56 ± 0.16*,†
Total	–	–	–	2.43 ± 0.22*	–	9.39 ± 0.23*,†

Abbreviations see text. Values for all glucosinolate species measured are given in Supplemental Table S4

n.d.: not detectable

* $p < 0.01$ in a statistical *t* test between Col-0 and the mutants

† $p < 0.01$ between *bcat4-2/bcat6-1* and *bcat3-1/bcat4-2/bcat6-1*

Table 5 Seed glucosinolate levels in different *bcat* mutants

Glucosinolate	Glucosinolate content in seeds (µmol/g)					
	Col-0	*bcat6-1*	*bcat4-2*	*bcat3-1*	*bcat4-2/bcat6-1*	*bcat3-1/bcat4-2/bcat6-1*
Met-derived						
2MSOE	n. d.	n. d.	n. d.	n. d.	1.18 ± 0.87*	1.20 ± 0.18*
3BZO	4.38 ± 0.44	4.76 ± 0.51	3.97 ± 1.30	5.33 ± 1.03	1.31 ± 0.25*	0.31 ± 0.05*,†
4OHB	4.86 ± 0.50	4.23 ± 0.38	3.63 ± 0.22*	4.54 ± 0.73	2.99 ± 0.65*	0.80 ± 0.09*,†
4BZO	16.67 ± 1.33	13.36 ± 0.94*	21.09 ± 2.23*	13.97 ± 0.88*	11.43 ± 5.67	1.42 ± 0.26*,†
4MTB	20.82 ± 3.04	24.62 ± 3.12	21.07 ± 4.37	34.32 ± 6.34*	6.35 ± 1.71*	0.85 ± 0.11*,†
7MTH	7.82 ± 0.57	9.47 ± 1.12*	2.42 ± 1.51*	11.55 ± 2.76*	0.58 ± 0.12*	0.29 ± 0.15*,†
8MTO	9.65 ± 0.43	11.43 ± 1.04*	3.62 ± 1.29*	9.21 ± 1.53	2.10 ± 0.31*	0.99 ± 0.16*,†
8MSOO	8.45 ± 0.72	10.39 ± 1.45*	5.62 ± 1.48*	11.81 ± 2.89	2.74 ± 0.30*	1.14 ± 0.10*,†
total	78.75 ± 6.06	85.13 ± 7.85	67.28 ± 11.51	112.81 ± 18.46	36.89 ± 5.48*	11.34 ± 0.77*,†
Leu-derived						
5MH	n. d.	n. d.	1.21 ± 0.00	n. d.	1.33 ± 1.76	2.72 ± 0.29*

4OHB, 4-hydroxybutylglucosinolate, other abbreviations are given in the text

n.d.: not detectable

* $p < 0.01$ in a statistical *t* test between Col-0 and the mutants

† $p < 0.01$ between *bcat4-2/bcat6-1* and *bcat3-1/bcat4-2/bcat6-1*

such an additive effect was seen for Met and Asn (Table 3, Supplemental Table S4). A strikingly different pattern of change was seen for SMM. This storage form of Met was undetectable in the *bcat6-1* mutant and in wild type, accumulated to about 0.5 µmol/g seed in *bcat4-2*, and was found at an amount three times higher in the *bcat4-2*/*bcat6-1* dko (1.54 µmol/g).

Cumulative effects on the levels of glucosinolates were seen in the *bcat4-2*/*bcat6-1* dko. In leaves, the total amount of Met-derived glucosinolates was found to be decreased to 43 % of wild-type level mainly due to the reduction of the major leaf glucosinolate species 4-methylsulfinylbutylglucosinolate (4MSOB), which is lowered to 50 % of wild-type level (Table 4, Supplemental Table S5). Both total Met-derived glucosinolates and 4MSOB were reduced to only 53 and 60 % of wild-type, respectively, in the *bcat4-2* mutant demonstrating the enhancing effect of the *bcat6-1* knockout and also confirming the major role of BCAT4 in the Met elongation pathway (Schuster et al. 2006).

An intriguing influence on glucosinolate concentrations was also seen in seeds. In the *bcat4-2*/*bcat6-1* dko, the total amount of Met-derived glucosinolates was reduced to approximately 47 % of the wild-type control, which is a further reduction with respect to *bcat4-2,* where this glucosinolate group was lowered to only 85 % of control (Table 5, Supplemental Table S6). The strong reduction in the dko is linked mainly to a reduction in 4-methylthiobutylglucosinolate (4MTB), the predominant glucosinolate species in seeds, but also to other glucosinolates that show stronger reductions in the dko than in the *bcat4-2* single mutant (3-benzoyloxypropylglucosinolate (3BZO), 6-methylsulfinylhexylglucosinolate (6MSOH), 7-methylthioheptylglucosinolate and 8-methylsulfinyloctylglucosinolate). Strikingly, 2-methylsulfinylethylglucosinolate (2MSOE), a glucosinolate species synthesized directly from Met without chain elongation, and 5-methylhexylglucosinolate (5MH), which derives from Val or Leu and not from Met, accumulate in the *bcat4-2*/*bcat6-1* dko. While 2MSOE was not seen in the *bcat4-2* single mutant, 5-methylhexylglucosinolate was found at reduced levels also in seeds of such plants (Table 5, Supplemental Table S6).

We also established a triple knockout (tko) mutant, which in addition to *bcat6-1* and *bcat4-2* contains the *bcat3-1* knockout allele (Knill et al. 2008). These plants (*bcat3-1*/*bcat4-2*/*bcat6-1)* exhibited a clear macroscopic phenotype with smaller rosettes and inflorescences in comparison to wild type. In addition, there were dent-like cavities and chlorotic areas in the leaves (Fig. 2). In this tissue, free amino acid profiling revealed that Ala, Arg, His, Ile, Phe, Pro Thr, Trp and Tyr showed moderately increased levels in comparison to the *bcat4-2*/*bcat6-1* dko or to the *bcat4-2* single mutants (Supplemental Table S3). Leu was found to be increased about twofold in the tko, whereas Val was significantly reduced in the triple mutant, which is linked to the knockout of BCAT3 and its role in the biosynthesis of this amino acid (Table 2, Supplemental Table S3) (Knill et al. 2008). Most striking is the extraordinary enhanced accumulation of Met, which is at 46-fold higher levels than in wild type and about eightfold higher than in the *bcat4-2*/*bcat6-1* dko or in the *bcat4-2* plants (Table 2, Supplemental Table S3). Substantial changes were also seen in seeds, where total free amino acids were doubled in comparison to all other lines investigated. The increase affected all amino acids and was found to be particularly strong in comparison to wild type for His (× 14.9), Ile (× 7.8), Thr (× 6.0), Arg (× 5.8) and was accompanied by a massive enrichment of SMM (Table 3, Supplemental Table S4).

Clear alterations in glucosinolate levels were observed in the leaves of the tko mutant. The total amount of Met-derived glucosinolates is threefold decreased with the most dramatic reduction seen for the major leaf glucosinolate 4MSOB, which was lowered to 25 % of the wild-type level (Table 4, Supplemental Table S5). In contrast, the levels of Leu-derived glucosinolates were strikingly enhanced with 5-methylhexylglucosinolate being extraordinarily enriched (× 9.8 in comparison to *bcat3-1*). Likewise, strong effects were measured in seeds. In this tissue, the level of total Met-derived glucosinolates was down to 14 % of the wild-type control, the two major glucosinolate species 4-methylthiobutylglucosinolate and 4-benzoyloxybutylglucosinolate being reduced to 4 and 7 % of wild-type, respectively. Slightly increased or unchanged amounts were detected for 5-methylsulfinylpentylglucosinolate (5MSOP), 5-methylthiopentylglucosinolate (5MTP) and 2MSOE. The opposing trend found in the levels of these glucosinolate species might be due to distinct substrate preferences in reactions of the second and third phase of glucosinolate biosynthesis. In addition, the substrate preference of glucosinolate transporter might influence the levels of individual compound in seeds (Nour-Eldin et al. 2012). Similar to leaves, 5-methylhexylglucosinolate was almost doubled in comparison to the *bcat3-1* and to the *bcat4-2*/*bcat6-1* dko mutants, whereas 4-methylpentylglucosinolate (4MP) was undetectable in this tissue (Table 5, Supplemental Table S6).

Collectively these metabolite profiling data revealed that the knockout of BCAT6 in conjunction with the cytosolic BCAT4 and the plastid-located BCAT3 caused a dramatic increase in Met content, coupled with clear reductions in Met-derived glucosinolates both in leaves and seeds. These deviations suggested that BCAT6 contributes to the biosynthesis of Met-derived glucosinolates. Among the branched-chain amino acids only Val was distinctively increased in the dko, while in the tko, Val was present at levels even lower than in wild type (Table 2).

Table 6 Content of various metabolites in foliage of *bcat* mutants

	Other metabolites in leaves					
	Col-0	*bcat6-1*	*bcat4-2*	*bcat3-1*	*bcat4-2/bcat6-1*	*bcat3-1/bcat4-2/bcat6-1*
Amino acid	Amino acid content in leaves (nmol/g dry weight)					
Leu	334.9 ± 23.0	279.6 ± 34.0*	311.3 ± 35.0	443.9 ± 39.4*	318.9 ± 23.2	702.3 ± 69.7*,†
Homo-Leu	n. d.	n. d.	n. d.	70.9 ± 13.1	n. d.	225.0 ± 34.3,†
Dihomo-Leu	n. d.	n. d.	n. d.	154.4 ± 19.4	n. d.	568.4 ± 72.1,†
Trihomo-Leu	n. d.	n. d.	2.5 ± 0.5	61.1 ± 6.2	2.4 ± 0.3	747.7 ± 90.4,†
Metabolite	Relative content (Peak area × 1000)					
5MTA	131.1 ± 13.3	112.3 ± 12.6	186.3 ± 25.5*	59.5 ± 5.8*	209.1 ± 11.7*	139.8 ± 13.6,†

n.d.: not detectable

* $p < 0.01$ in a statistical *t* test between Col-0 and the mutants

† $p < 0.01$ between *bcat4-2/bcat6-1* and *bcat3-1/bcat4-2/bcat6-1*. Abbreviations see text

Table 7 Levels of diverse compounds in seeds of different *bcat* mutants

	Other metabolites in seeds					
	Col-0	*bcat6-1*	*bcat4-2*	*bcat3-1*	*bcat4-2/bcat6-1*	*bcat3-1/bcat4-2/bcat6-1*
Metabolite	Relative content (Peak area × 1000)					
5BZO-NH2	1.5 ± 0.9	4.4 ± 2.5	1849.9 ± 2944.9	11.4 ± 2.5*	6080.0 ± 1602.4*	2717.1 ± 1172.6*,†
5MTA	2.2 ± 0.3	2.6 ± 0.4	8.0 ± 7.3*	3.7 ± 0.7*	15.6 ± 11.1*	61.5 ± 9.1*,†

* $p < 0.01$ in a statistical *t* test between Col-0 and the mutants

† $p < 0.01$ between *bcat4-2/bcat6-1* and *bcat3-1/bcat4-2/bcat6-1*. Abbreviations see text

BCAT inactivation leads to increases in an intermediate of a Met salvage pathway

Apart from amino acid and glucosinolate profiling we used a LC-ESI-TripleQuad-MS method employing an LC-ESI-IonTrap to search for other compounds that differed among the single, double and triple mutants. In leaves of the *bcat4-2* and *bcat3-1* single and the dko, and especially in the tko, we detected elongated Leu derivatives. These amino acids were detected in about three to tenfold higher amounts in the tko than in any other line, and trihomoleucine was found in the range of Leu (Table 6). The *bcat3-1* mutant also contained considerable amounts of homo-, dihomo- and trihomoleucine, but only trace amounts of trihomoleucine were found in *bcat4-2* and in the *bcat4-2/bcat6-1* dko. None of these abnormal Leu derivatives was detectable in seeds.

The relative levels of 5′-deoxy-5′-methylthioadenosine (5MTA), an intermediate of the Met recycling pathway (Bürstenbinder et al. 2010; Miyazaki and Yang 1987) were highest in the leaves of the *bcat4-2* single and the *bcat4-2/bcat6-1* dko (Table 6). In seeds, the highest relative amounts of 5MTA were found in the tko, with a 28-fold increase observed relative to wild-type levels. The double mutant also exhibited sevenfold increase, whereas only moderate elevation were found in all single mutants, maximally 3.6-fold in *bcat4-2* (Table 7). In contrast, 5MTA is reduced in leaves of the *bcat3-1* knockout mutant. Besides 5MTA we also found extremely enhanced levels of 1-amino-5-benzoyloxypentane (5BZO-NH2 could potentially originate from 5-benzoyloxypentylglucosinolate) in seeds of the *bcat4-2* (1200-fold increase), the dko (over 4000-fold increase) and the tko (a near 1800-fold increase). Only very moderate increases were found in the *bcat6-1* and in the *bcat3-1* mutant (Table 7). 5BZO-NH2 was not detected in green tissues.

Expression of BCAT6

Considering the potential role of BCAT6 in glucosinolate metabolism we used previously established Arabidopsis lines containing *BCAT6*-promoter:GUS constructs, to reinvestigate expression of *BCAT6* in different developmental stages carrying out histological staining in the presence of 0.05 % Silwet Top for increased sensitivity. Studies of seedlings now revealed promoter activity in the central cylinder throughout the root and the hypocotyl with particularly strong staining in the root tip and at the upper end of the hypocotyl at the basis of the petioles of cotyledons, where promoter activity was previously detected (Supplemental

Fig. S5) (Schuster and Binder 2005). In later developmental stages, staining was now seen at the basis of petioles and in stipules. Consistent with former studies, promoter activity was seen in anthers and root tips, whereas no promoter activity was detected in other parts of the leaves even after wounding. Furthermore no staining was detectable in imbibed seeds (not shown). Taken together BCAT6 promoter activity is restricted to seedling stages and to small regions of the adult plants.

Discussion

Arabidopsis contains two cytosolic branched-chain aminotransferases

The Arabidopsis genome encodes six transcribed branched-chain aminotransferase genes (*BCAT1* to *BCAT6*) and a pseudo-gene (*BCAT7*), for which no transcripts had been detected (Diebold et al. 2002). Two genes each encode mitochondria-located (BCAT1 and 2) and chloroplast-localized (BCAT3 and 5) branched-chain aminotransferases (Angelovici et al. 2013; Diebold et al. 2002; Zybailov et al. 2008). Now our YFP and GFP tagging experiments in tobacco protoplasts and in transgenic Arabidopsis plants demonstrated that there are also two cytosolic BCATs in this model species. The distribution of the fluorescence within the cell is different from that of the vacuole-located SlBCAT6 in cultivated tomato (Maloney et al. 2010), suggesting that Arabidopsis does not contain a BCAT in this hydrolytic compartment. The cytosolic localization of BCAT6 is further supported by the very similar structure of this protein and the cytosolic BCAT4, both lacking N-terminal extensions. In addition, we never observed any hints for localization of BCAT6 or any other BCAT in peroxisomes. There is no C-terminal localization signal present in these proteins, and none of these enzymes has been detected in proteomic studies of these organelles suggesting that BCATs are absent from peroxisomes (Eubel et al. 2008; Kaur and Hu 2011; Reumann et al. 2009). In the light of several hints about a role of this subcellular compartment in Val degradation (Binder 2010; Kauer et al. 2009), it appears that these organelles contain either other aminotransferases that accept branched-chain amino acids as substrates or that the corresponding 2-oxo acid or other Val degradation pathway intermediates are imported into these organelles for further metabolism. In the latter case, cytosolic branched-chain aminotransferases might catalyze the first catabolic step generating 3MOB. Whereas BCAT4 did not show any activity with Val and its 2-oxo acid 3MOB, BCAT6 exhibits activities with all BCAAs and their corresponding 2-oxo acids suggesting this enzyme to be a candidate for a role in degradation of Val. However, only a slightly significant increase of Val was detectable in leaves of the *bcat4-2*/*bcat6-1* dko mutant (Table 2), and no changes were seen in both single mutants. Thus a role of BCAT6 in amino acid catabolism remains unclear, despite the substantial activity of this enzyme with all BCAAs and the corresponding 2-oxo acids. The activity with Met and MTOB suggests a potential function of BCAT6 in the Met chain elongation pathway.

Knockout of both cytosolic BCATs leads to strong effects on glucosinolate accumulation

A strong impact of the *bcat4-2*/*bcat6-1* dko was observed on the metabolism of Met-derived glucosinolates and related compounds. In both leaves and seeds, the inactivation of both genes enhanced the already strong reductions in the total levels of Met-derived glucosinolates seen in the *bcat4-2* mutant, although the knockout of BCAT6 alone appeared to have no substantial impact on the accumulation of this group of specialized compounds (Tables 4, 5). The absence of detectable changes in glucosinolate and amino acid content might be related to the restricted expression of the *BCAT6* gene in particular tissues of adult plants (Supplemental Fig. S5).

In the dko, there were both reductions and also some increases in glucosinolate species of different chain lengths. Interestingly, 2-methylsulfinylethylglucosinolate (2MSOE) accumulated in seeds of the dko, but was undetectable in both single mutants. This glucosinolate species is synthesized directly from Met without chain elongation. Its formation is unexpected considering that both aldoxime forming enzymes of aliphatic glucosinolate biosynthesis, CYP79F1 and CYP79F2, show in vitro activity only with chain-extended Met homologs but not with Met and thus Met might also be a poor substrate for these enzymes in vivo explaining the relatively low amounts of this glucosinolate species in dko (Chen et al. 2003; Hansen et al. 2001). The formation of 2MSOE may be driven by high concentrations of Met in distinct tissues or cells. We did not see a further increase of 2MSOE in the triple mutant, in which almost all free amino acids were increased in comparison to the dko including a modest elevation of Met and a marked increase of SMM. It might be possible that the knockout of both BCAT4 and BCAT6 leads to a particular increase in cytosol-located Met that might directly be available for glucosinolate core biosynthesis. Our previous observation that 2MSOE also accumulates in seeds of a *bcat3-1*/*bcat4-2* dko mutant, may have the same cause (Knill et al. 2008). BCAT3 is located in plastids and is predominantly involved in Val biosynthesis. While its single knockout provokes only moderate increases of Ser, Thr and Val in leaves, the double knockout of BCAT3 and BCAT4 s leads to an extraordinary increase of total amino acids in

seeds. This might also include a rise of the cytosolic Met level, which would be the trigger for 2MSOE production. Since glucosinolates are not synthesized in seeds the conversion of Met into 2MSOE has to occur in other tissues, such as siliques that harbor the enzymatic equipment required for glucosinolate core structure formation (Brown et al. 2003; Nour-Eldin et al. 2012). In seeds of the *bcat3-1/bcat4-2* dko mutant, a considerable amount of free Met is converted to SMM which is markedly increased. Similar to the formation of 2MSOE, the accumulation of 4-methylpentylglucosinolate and 5-methylhexylglucosinolate can be considered to be a consequence of an imbalance in free BCAAs (Knill et al. 2008). The massive increase of these Leu-derived glucosinolates in the tko might be explained by the following scenario. As demonstrated previously for isopropylmalate isomerase, Leu biosynthesis and the first and second cycle of the Met chain elongation pathway involve the same proteins (Imhof et al. 2014). By reducing the cytosolic formation of the 2-oxo acid MTOB from Met, the double knockout of *BCAT4* and *BCAT6* might free up catalytic capacity for elongation of other 2-oxo-acids such as 3 MOP or 3 MOB. As a consequence, 5-methylhexylglucosinolate is formed from the elongation of Leu accumulates in the seeds of *bcat4-2*, the dko and the tko (Table 5). The additional knockout of BCAT3 in the tko shuts down Val biosynthesis and thus increases the flux towards Leu resulting in further enhanced quantities of Leu derivatives and Leu-derived glucosinolates also in green tissue (Tables 4, 6). The differential accumulation of these Leu-derived compounds in leaves and seeds might be explained by the general differences among the amino acid metabolism in these tissues (Fait et al. 2006), but might be also linked to distinct substrate specificities of the transporters that translocate glucosinolates into the phloem (Nour-Eldin et al. 2012).

In contrast to 2MSOE, the levels of total Met-derived glucosinolates are highly reduced in seeds and leaves of the tko. In leaves, this is mainly due to the reduction of the main glucosinolate species 4MSOB, whereas in seeds several glucosinolate species show additional decreases in comparison to the dko mutant. Most strikingly, the leaf Met level is massively increased in the tko in comparison to both wild type (× 46) and to the dko (× 8), demonstrating that only a small part of the free Met is converted to 2MSOE. This might be related to the compartmentalization of the Met pool in specific tissues, cells or sub-cellular locations.

The reason for the macroscopic phenotype of the triple mutant remains unclear at present. Retarded growth may be attributed to the knockout of *BCAT3*, since impaired growth and development were already seen in the single mutant. However, the aberrant leaf phenotype remains mysterious and does not resemble any symptoms observed upon the knockdown of small subunit 1 of isopropylmalate isomerase, an enzyme involved in the chain elongation of Leu and C3 and C4 Met-derived glucosinolates (Imhof et al. 2014).

Cytosolic BCATs may be involved in methionine salvage and glucosinolate hydrolysis

The knockout of both cytosolic BCATs has a strong influence on the steady state levels of Met and Met-derived compounds such as SMM, 2MSOE and the Met salvage intermediate 5MTA from which Met can be recovered. In the dko mutant, the strong accumulation of 5MTA correlates with lowered levels of Met-derived glucosinolates and consequently with a lowered demand for MTOB, which is generated from 5MTA in the Met salvage pathway. Thus the increase of 5MTA might indicate that MTOB recovered from the recycling pathway is directly channeled into glucosinolate biosynthesis without first being reaminated to Met. This is independent from the activity of BCAT4 and/or BCAT6 in the initial deamination of Met strongly suggesting that impaired glucosinolate biosynthesis in *bcat4-2* and *bcat4-2/bcat6-1* plants seems to be also caused by a deficiency in the amination reactions converting chain elongated 2-oxo acids to Met derivatives. In leaves of *bcat3-1*, 5MTA is reduced to about 50 % of wild-type level possibly due to higher rate of glucosinolate biosynthesis as indicated by an enrichment of these metabolites in seeds, although in this tissue 5MTA is slightly elevated in comparison to wild-type (Tables 5, 6, 7).

In seeds, we also observed a relatively strong accumulation of 5BZO-NH2 with highest levels found in the dko (×4053), the tko (×1811) and *bcat4-2* (×1233). This compound might be a hydrolysis product of 5-benzoyloxypentylglucosinolate (5BZO), a low abundant glucosinolate species found in seeds of Arabidopsis (Hogge et al. 1988; Knill et al. 2008). The unusual accumulation of this amine seems to be a result of the *bcat4-2* knockout allele, but is clearly enhanced by the additional knockout of BCAT6 (Table 7). In contrast, the additional knockout of BCAT3 reduces the level of this amine to about 50 % of the amount found in the dko. An amine derived from another glucosinolate, the indolic indol-3-ylmethylglucosinolate (I3M) was found as pathogen-induced compound in Arabidopsis, and the generation of this amine depends on the function of an atypical myrosinase (PEN2). This I3M-derived amine and amines derived from the aliphatic glucosinolates 4MSOB and 3MSOP were detected upon the ectopic expression of the myrosinase TGG4 (Bednarek et al. 2009; Wittstock and Burow 2010). These observations support the hypothesis that 5BZO-NH2 is indeed a breakdown product of the corresponding glucosinolate species, which is usually present in rather low amounts. The loss of BCAT4 and BCAT6 may favor the generation of 5BZO, which is subsequently

converted into 5BZO-NH2. Such a conversion would require a highly specific β-thioglucoside glucohydrolase similar to PEN2 as mentioned above.

Another explanation for the occurrence of 5BZO-NH2 might be that lines carrying the *bcat4-2* knockout allele exhibit an enhanced susceptibility to pathogens due to altered levels or changes in glucosinolate composition leading to infection and the accumulation of this pathogen-induced amine. However, none of the plants in this study exhibited any other indications of pathogen infection.

Residual glucosinolate synthesis in the tko

The knockout of BCAT6, BCAT4 and BCAT3 severely impaired the biosynthesis of Met-derived glucosinolates. Nevertheless a residual amount of this class of specialized metabolites still accumulated in the tko plants. This raises the question of which other aminotransferases are able to support transamination reactions required for Met chain elongation. The plastid-located BCAT5 is a candidate, although the knockout of this gene does not have any significant influence on glucosinolate biosynthesis. Nevertheless, a double knockout of BCAT4 and BCAT5 results in a reduction of 8-methylsulfinyloctylglucosinolate and increases of Met and SMM supporting a potential role of BCAT5 in Met chain elongation (M. Lackner, J. Imhof, M. Reichelt, J. Gershenzon and S. Binder, unpublished results). However, considering the very low expression of BCAT5 it is likely that still other aminotransferases have the potential to support Met chain elongation and the biosynthesis of Met-derived glucosinolates.

Acknowledgments We thank Ulrike Tengler and Conny Guha for excellent technical assistance. We are also grateful to Laura Maccarone and Sarah Kovarik for their engagement in subcellular localization studies. This work was supported by Grant Bi 590/9-2 from the Deutsche Forschungsgemeinschaft.

References

Angelovici R, Lipka AE, Deason N, Gonzalez-Jorge S, Lin H, Cepela J, Buell R, Gore MA, Dellapenna D (2013) Genome-wide analysis of branched-chain amino acid levels in *Arabidopsis* seeds. Plant Cell 25:4827–4843

Bednarek P, Piślewska-Bednarek M, Svatoš A, Schneider B, Doubský J, Mansurova A, Humphry M, Consonni C, Panstruga R, Sanchez-Vallet A, Molina A, Schulze-Lefert P (2009) A glucosinolate metabolism pathway in living plant cells mediates broad-spectrum antifungal defense. Science 323:101–106

Binder S (2010) Branched-chain amino acid metabolism in *Arabidopsis thaliana.* Arabidopsis Book 8:e0137. doi:10.1199/tab.0137

Brown PD, Tokuhisa JG, Reichelt M, Gershenzon J (2003) Variation of glucosinolate accumulation among different organs and developmental stages of *Arabidopsis thaliana*. Phytochemistry 62:471–481

Bürstenbinder K, Waduwara I, Schoor S, Moffatt BA, Wirtz M, Minocha SC, Oppermann Y, Bouchereau A, Hell R, Sauter M (2010) Inhibition of 5′-methylthioadenosine metabolism in the Yang cycle alters polyamine levels, and impairs seedling growth and reproduction in Arabidopsis. Plant J 62:977–988

Chen S, Glawischnig E, Jorgensen K, Naur P, Jorgensen B, Olsen CE, Hansen CH, Rasmussen H, Pickett JA, Halkier BA (2003) CYP79F1 and CYP79F2 have distinct functions in the biosynthesis of aliphatic glucosinolates in *Arabidopsis*. Plant J 33:923–937

Clough SJ, Bent AF (1998) Floral dip: a simplified method for Agrobacterium-mediated transformation of *Arabidopsis thaliana*. Plant J 16:735–742

Diebold R, Schuster J, Däschner K, Binder S (2002) The branched-chain amino acid transaminase gene family in *Arabidopsis* encodes plastid and mitochondrial proteins. Plant Physiol 129:540–550

Docimo T, Reichelt M, Schneider B, Kai M, Kunert G, Gershenzon J, D'Auria JC (2012) The first step in the biosynthesis of cocaine in *Erythroxylum coca*: the characterization of arginine and ornithine decarboxylases. Plant Mol Biol 78:599–615

Edwards K, Johnstone C, Thompson C (1991) A simple and rapid method for the preparation of plant genomic DNA for PCR analysis. Nucleic Acids Res 19:1349

Eubel H, Meyer EH, Taylor NL, Bussell JD, O'Toole N, Heazlewood JL, Castleden I, Small ID, Smith SM, Millar AH (2008) Novel proteins, putative membrane transporters, and an integrated metabolic network are revealed by quantitative proteomic analysis of *Arabidopsis* cell culture peroxisomes. Plant Physiol 148:1809–1829

Fait A, Angelovici R, Less H, Ohad I, Urbanczyk-Wochniak E, Fernie AR, Galili G (2006) Arabidopsis seed development and germination is associated with temporally distinct metabolic switches. Plant Physiol 142:839–854

Halkier BA, Gershenzon J (2006) Biology and biochemistry of glucosinolates. Annu Rev Plant Biol 57:303–333

Hansen CH, Wittstock U, Olsen CE, Hick AJ, Pickett JA, Halkier BA (2001) Cytochrome P450 CYP79F1 from arabidopsis catalyzes the conversion of dihomomethionine and trihomomethionine to the corresponding aldoximes in the biosynthesis of aliphatic glucosinolates. J Biol Chem 276:11078–11085

Hogge LR, Reed DW, Underhill EW (1988) HPLC separation of glucosinolates from leaves and seeds of Arabidopsis thaliana using thermospray liquid chromatopgraphy-mass spectrometry. J Chromatogr Sci 26:551–556

Imhof J, Huber F, Reichelt M, Gershenzon J, Wiegreffe C, Lächler K, Binder S (2014) The small subunit 1 of the Arabidopsis isopropylmalate isomerase is required for normal growth and development and the early stages of glucosinolate formation. PLoS ONE 9:e91071

Kaur N, Reumann S, Hu J (2009) Peroxisome biogenesis and function. Arabidopsis Book 7:e0123. doi:10.1199/tab.0123

Kaur N, Hu J (2011) Defining the plant peroxisomal proteome: from *Arabidopsis* to rice. Front Plant Sci 2:103

Knill T, Schuster J, Reichelt H, Gershenzon J, Binder S (2008) Arabidopsis branched-chain aminotransferase 3 functions in both amino acid and glucosinolate biosynthesis. Plant Physiol 146:1028–1039

Knill T, Reichelt H, Paetz C, Gershenzon J, Binder S (2009) *Arabidopsis thaliana* encodes a bacterial-type heterodimeric isopropylmalate isomerase involved in both Leu biosynthesis and the Met chain elongation pathway of glucosinolate formation. Plant Mol Biol 71:227–239

Maloney GS, Kochevenko A, Tieman DM, Tohge T, Krieger U, Zamir D, Taylor MG, Fernie AR, Klee HJ (2010) Characterization of

the branched-chain amino acid aminotransferase enzyme family in tomato. Plant Physiol 153:925–936

Matthes A, Schmidt-Gattung S, Köhler D, Forner J, Wildum S, Raabe M, Urlaub H, Binder S (2007) Two DEAD-box proteins may be part of RNA-dependent high-molecular-mass protein complexes in Arabidopsis mitochondria. Plant Physiol 145:1637–1646

Miyazaki JH, Yang SF (1987) The methionine salvage pathway in relation to ethylene and polyamine biosynthesis. Physiol Plant 69:366–370

Nour-Eldin HH, Andersen TG, Burow M, Madsen SR, Jorgensen ME, Olsen CE, Dreyer I, Hedrich R, Geiger D, Halkier BA (2012) NRT/PTR transporters are essential for translocation of glucosinolate defence compounds to seeds. Nature 488:531–534

Ranocha P, McNeil SD, Ziemak MJ, Li C, Tarczynski MC, Hanson AD (2001) The *S*-methylmethionine cycle in angiosperms: ubiquity, antiquity and activity. Plant J 25:575–584

Reumann S, Quan S, Aung K, Yang P, Manandhar-Shrestha K, Holbrook D, Linka N, Switzenberg R, Wilkerson CG, Weber AP, Olsen LJ, Hu J (2009) In-depth proteome analysis of *Arabidopsis* leaf peroxisomes combined with in vivo subcellular targeting verification indicates novel metabolic and regulatory functions of peroxisomes. Plant Physiol 150:125–143

Sambrook J, Russell DW (2001) Molecular Cloning: A Laboratory Manual. Cold Spring Harbor Laboratory Press, Cold Spring Harbor, NY

Sauter M, Moffatt B, Saechao MC, Hell R, Wirtz M (2013) Methionine salvage and *S*-adenosylmethionine: essential links between sulfur, ethylene and polyamine biosynthesis. Biochem J 451:145–154

Schuster J, Binder S (2005) The mitochondrial branched-chain aminotransferase (AtBCAT-1) is capable to initiate degradation of leucine, isoleucine and valine in almost all tissues in *Arabidopsis thaliana*. Plant Mol Biol 57:241–254

Schuster J, Knill T, Reichelt H, Gershenzon J, Binder S (2006) BRANCHED-CHAIN AMINOTRANSFERASE 4 is part of the chain elongation pathway in the biosynthesis of methionine-derived glucosinolates in *Arabidopsis*. Plant Cell 18:1–16

Singh BK (1999) Biosynthesis of valine, leucine and isoleucine. In: Singh BK (ed) Plant amino acids: biochemistry and biotechnology. Marcel Dekker, New York, pp 227–247

Tzfira T, Tian GW, Lacroix B, Vyas S, Li J, Leitner-Dagan Y, Krichevsky A, Taylor T, Vainstein A, Citovsky V (2005) pSAT vectors: a modular series of plasmids for autofluorescent protein tagging and expression of multiple genes in plants. Plant Mol Biol 57:503–516

Weigel D, Glazebrook J (2002) Arabidopsis, a laboratory manual. Cold Spring Harbor Laboratory Press, Cold Spring Habor, NY

Wittenbach VA, Abell LM (1999) Inhibitors of valine, leucine and isoleucine biosynthesis. In: Singh BK (ed) Plant amino acids: biochemistry and biotechnology. Marcel Dekker, New York, pp 385–416

Wittstock U, Burow M (2010) Glucosinolate breakdown in Arabidopsis: mechanism, regulation and biological significance. Arabidopsis Book 8:e0134. doi:10.1199/tab.0134

Wittstock U, Halkier BA (2002) Glucosinolate research in the *Arabidopsis* era. Trends Plant Sci 7:263–270

Zybailov B, Rutschow H, Friso G, Rudella A, Emanuelsson O, Sun Q, van Wijk KJ (2008) Sorting signals, N-terminal modifications and abundance of the chloroplast proteome. PLoS ONE 3:e1994